Shape Memory Polyurethanes from Renewable Polyols Obtained by ATMET Polymerization of Glyceryl Triundec-10-enoate and 10-Undecenol

Enrique del Río, Gerard Lligadas, Juan Carlos Ronda, Marina Galià, Virginia Cádiz, Michael A. R. Meier

Abstract: The synthesis of branched polyols from glyceryl triundec-10-enoate by acyclic triene metathesis polymerization (ATMET) is reported. 10-Undecenol is used as a monofunctional comonomer to end-cap polymer chains, functionalize the periphery of the resulting branched materials, and to control the molecular weight. The thus obtained castor oil derived polyols are reacted with 4,4'-methylenebis(phenylisocyanate) (MDI) to yield a series of semicrystalline polyurethane networks. The investigation of the thermal stability and the thermomechanical and mechanical properties of these thermosets revealed good shape memory properties.

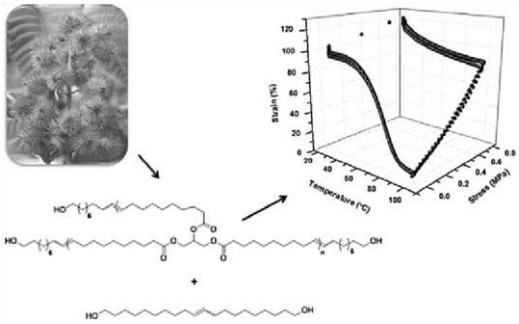

Introduction

In recent years, the utilization of renewable raw materials, such as plant oils and natural fatty acids, for replacing petroleum derived raw materials for the production of polymeric materials has attracted great attention.[1] The main components of vegetable oils are triglycerides, which are the product of esterification between a molecule of glycerol and three fatty acids. Many of these fatty acids have double bond functional groups in the aliphatic chain, which, in combination with the development of olefin metathesis,[2] offers manifold new possibilities for the utilization of these renewable resources for organic and polymer chemists.[3] The polymer field has probably benefited most from this development by applying metathesis chemistry for the synthesis of renewable monomers[4] for step-growth polymerizations and the possibility to polymerize plant oil based α,ω-dienes via acyclic diene metathesis (ADMET) polymerization.[5] Moreover, ADMET was shown to be an efficient tool for the synthesis of a wide variety of linear polymers and polymer architectures that are not available using other polymerization methods.[6] It has been demonstrated that ADMET polymerization can proceed in the presence of heteroatoms as long as the terminal olefins are far enough apart from them.[7] Many examples of ADMET of heteroatom-containing α,ω-dienes exist in the literature, since the introduction of functionalities to the backbone of a polymers provides different properties and permits further modifications.[8] The development of ADMET polymerization and the possibility to control the polymer molecular weight using chain stoppers has opened new possibilities to obtain desired polymer architectures.[9] Moreover, chain stopper strategies have recently been exploited with the aim of polymerizing monomers with functionalities higher than two in order to avoid cross-linking. The thus named acyclic triene metathesis (ATMET) polymerization has been used in order to obtain branched polymers. In this way, glyceryl triundec-10-enoate (1), synthesized from glycerol and methyl undec-10-enoate, was polymerized using methyl acrylate as chain stopper in presence of Hoveyda– Grubbs second generation catalyst. The relative amount of added methyl acrylate made it possible to tune the molecular weight of the hyperbranched polymers, to functionalize them in their periphery and to completely avoid their crosslinking.[10] This strategy has also been used with success in the ATMET polymerization of high oleic sunflower oil.[11]

In a previous work, we reported the ADMET polymerization of 1,3-di10-undecenoxy-2-propanol using 10undecenol as renewable comonomer to end-cap polymer chains and limit the molecular weight. The linear polyols obtained in this way were reacted with MDI to yield a series of amorphous and semicrystalline polyurethane networks that showed good shape memory properties.[12] Shape-memory materials can be deformed and fixed into a temporary shape, and afterward recover their original and permanent shape by exposure to an external stimulus.[13,14] Most commonly, heat or light have been used as stimulus for shape memory polymers

(SMPs).[15] Moreover, the indirect actuation of the shape memory effect has also been carried out by using irradiation with infrared light, application of electric fields, alternating magnetic fields, or immersion in water.[16] Applications of SMPs can be found, e.g., in heat-shrinkable tubes for electronics or films for packaging, self-deployable sun sails in spacecraft, intelligent medical devices, or implants for minimally invasive surgery.[17]

In this work, we focused on the synthesis of branched polyols to take advantage of their properties including lower viscosity and increased solubility, if compared to their linear analogs. We have used ATMET polymerization of 1 as trifunctional monomer and 10-undecenol 2 as chain stopper (see Scheme 1) to obtain branched polyols that are functionalized in their periphery. By varying the ratio between 1 and 2, it was possible to vary the molecular weight and hydroxyl number and to avoid cross-linking.

These polyols have been reacted with 4,4'-methylenebis(phenylisocyanate) (MDI) to obtain a series of polyurethanes that were characterized by infrared spectroscopy, differential scanning calorimetry (DSC), thermogravimetric analysis (TGA), and thermodynamic mechanical analysis (DMA). In this study, we also investigated the shape memory properties of these materials.

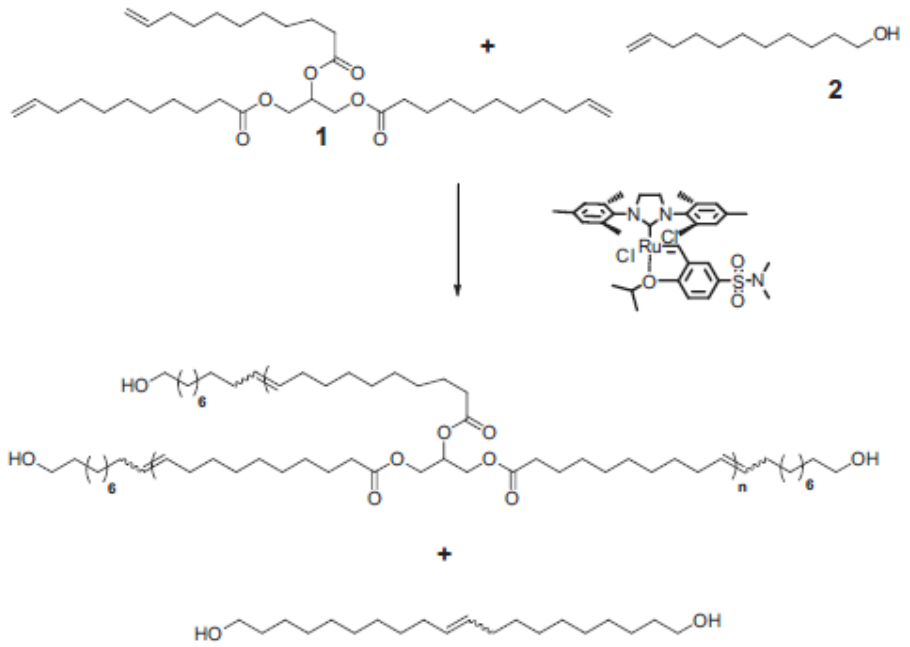

Scheme 1. Synthesis of branched polyols via ATMET of triglyceride **1** with chain stopper **2**.

Experimental Section

Materials

10-Undecenol, ethyl vinyl ether (EVE), benzylidene[1,3-bis(2,4,6trimethylphenyl)-2-imidazolidinylidene]-dichloro(tricyclohexylphosphine)-ruthenium (second generation Grubbs catalyst), [1,3-bis(2,4,6-trimethylphenyl)-2-imidazolidinylidene]-dichloro(o-isopropoxyphenylmethylene)ruthenium (second generation Hoveyda–Grubbs catalyst), [1,3-dimesityl-2-imidazolidinylidene]dichloro (phenylmethylene)bis(3-bromopyridine)-ruthenium(II) (third generation Grubbs catalyst), 1,3-bis(2,4,6-trimethylphenyl)4,5-dihydroimidazol-2-ylidene[2-(i-propoxy)-5-(N,N-dimethylaminosulfonyl)phenyl]-methyleneruthenium(II) dichloride (Zhan Catalyst), and MDI were supplied by Aldrich. Glyceryl triundec-10enoate (1) was synthesized following a previously reported method.[10]

Synthesis of the Polyols

Glyceryl triundec-10-enoate (1) and 10-undecenol (2) were introduced in a 3 mL conical vial in the desired molar ratio. The reaction was equipped with magnetic stirring and a screwcap with a septum. The mixture was homogenized at room temperature for 10 min, 0.3 mol-% of catalyst was added and the reaction was equipped with a N_2 purge and

heated at 50 ºC with stirring for 3 h. Then, a second portion of catalyst (0.1 mol-%) was added and the mixture was stirred for an additional 3 h at 80 ºC. The reaction was stopped by adding EVE in a 50:1 EVE/catalyst ratio.

^{1}HNMR ($CDCl_3$, TMS, 400 MHz): δ (ppm) = 5.45–5.30(m, CH=CH), 5.28–5.22 (m, $CH_2CH(O)CH_2$), 4.32–4.24 (dd, J = 4.5 and 12.0 Hz, OCH_2CH), 4.16–4.09 (dd, J = 6.0 and 11.8 Hz, OCH_2CH), 3.62 (t, J = 6.8 Hz, CH_2OH), 2.30 (t, J = 7.5 Hz, CH_2COO), 2.05–1.90 (m, CH_2CH=CH), 1.70–1.50 (m, CH_2CH_2–COO), 1.40–1.20 (m, aliphatic backbone), 0.95 (t, J = 7.2 Hz, =$CHCH_2CH_3$), 0.87 (t, J = 7.2 Hz, $CH_2CH_2CH_3$).

FTIR (cm^{-1}): 3370, 2923, 2852, 1744.

Determination of Hydroxyl Content

The milimol of hydroxy groups per gram of polymer was determined by 1H NMR spectroscopy using 2-phenylethanol as the internal standard (3.85 ppm). Primary hydroxyl content was determined from the signal centered at 3.62 ppm. The following equation was used:

$$\text{value OH} = \frac{\text{mmol IS} \times \text{Int POH}}{\text{Int IS} \times \text{gPOH}} \qquad (1)$$

where POH is the polyol, IS the internal standard, mmol IS the quantity of internal standard added to the sample in millimole, and gPOH is the quantity of sample measured in grams.

Synthesis of the Polyurethanes

Polyol was dissolved in anhydrous toluene (1:1 w/w) under argon atmosphere, heated to 50 ºC and added into a dispersion of MDI in toluene (1/1 w/w). The solution was homogenized and cast over a silanized glass preheated to 70 ºC. The polyurethane was maintained at 70 ºC for 2 h and at 120 ºC for 3 h.

FTIR (cm^{-1}): 3353, 2924, 2852, 1 738, 1596.

Instrumentation

^{1}H NMR (400 MHz) spectra were recorded in $CDCl_3$ using a Varian Gemini 400 spectrometer. Chemical shifts were reported in ppm relative to tetramethylsilane (TMS) and $CHCl_3$ as internal standards.

Calorimetric studies were carried out on a Mettler DSC822e thermal analyzer using N_2 as a purge gas (100 $mLmin^{-1}$) at a scan rate of 20 ºC min^{-1}. Thermal stability studies were carried out on a Mettler TGA/SDTA851e/LF/1100 with N_2 as the purge gas. The studies were performed in the 30–800 ºC temperature range at a heating rate of 10 ºC min^{-1}.

The IR spectra were recorded on a Bomem Michelson MB 100 FTIR spectrophotometer with a resolution of 4 cm^{-1} in the absorbance mode. An attenuated total reflection (ATR) accessory with thermal control and a diamond crystal (Golden Gate heated single-reflection diamond ATR, Specac-Teknokroma) was used to determine FTIR spectra.

Size exclusion chromatography (SEC) analysis was carried out with an Agilent 1200 series system with PLgel 3 µm MIXED-E, PLgel 5 µm MIXED-D, and PLgel 20 µm MIXED-A columns in series, and equipped with an Agilent 1100 series refractive-index detector. Calibration curves were based in polystyrene standards having low polydispersities. THF was used as an eluent at a flow rate of 1.0 mL min^{-1}, the sample concentrations were 5–10 mg mL^{-1}, and injection volumes of 100 mL were used.

Dynamic mechanical thermal analysis (DMTA), tensile tests properties and the shape-memory effect were measured with a TA DMA 2928 dynamic mechanical thermal analyzer. Specimens 0.6 mm thick, 3 mm wide, and 8 mm long were tested with a tension film clamp. For DMTA the temperature range was from –90 to 150 ºC, at a heating rate of 3 ºC min^{-1} and at a fixed frequency of 1 Hz. The tensile assays were performed by triplicate, measuring the strain while applying a stress ramp of 1 N min^{-1} at 25 ºC. The shape-memory effect was quantified in the controlled-force setup as follow the sample was equilibrated at 100 ºC and a force ramp of 0.5 N min^{-1} was applied until a determined stress (previously estimated by a stress–strain experiment at 100 ºC) to achieve the desired strain. Maintaining the stress applied, the sample was cooled down to 25 ºC at 10 ºC min^{-1} and equilibrated at this temperature for 10 min. Then, the stress was released and the temperature maintained at 25 ºC for 5 min. Finally, the temperature was increased at 5 ºC min^{-1} to 100 ºC. Three consecutive cycles were applied to each sample. Strain fixity and strain recovery ratios were measured for the three cycles.

Results and Discussion

The ATMET polymerization of 1inpresence of 10-undecenol 2 as chain stopper was carried out using a total of 0.4 mol-% of Zhan catalyst (Scheme 1). Grubbs second generation catalyst required the double amount of catalyst to achieve a similar degree of polymerization. Grubbs third generation and Hoveyda–Grubbs second generation catalysts showed rather low conversion for this reaction.

If the Zhan catalyst was added in one portion, the reaction mixture with the lowest proportion of chain stopper gave cross-linked byproducts. However, it was found that a stepwise addition of the catalyst provided a better control of the branching reaction avoiding crosslinking. Thus, in the first step, 0.3% of catalyst per mol of the total amount of double bonds was added and the reaction was heated to 50 ºC; three hours later a second batch of catalyst (0.1%) was added and the temperature was increased to 80 ºC and maintained for three more hours. Five polyols were thus synthesized by varying the 2:1 ratio (Table 1). As it is well known, metathesis polymerizations proceed with some migration of the terminal double bond to internal positions. Therefore, isomerized 10-undecenol was removed after the reaction by applying high vacuum at 70 ºC for 12 h. The resulting polyols were analyzed by SEC (Figure1)and thepercentageofself-metathesisof2(peakat 25 min in Figure 1) was found to increase while the molecular weights decreased with increasing ratios of 2:1. Thus, polyols with a smaller amount of chain stopper have higher molecular weight and higher polydispersity, which is in agreement with previously reported ATMET polymerization results.[10,11] One of the most important parameters of the polyols for the synthesis of polyurethanes is the amount and nature of hydroxyl groups. The synthesized polyols have only primary hydroxyl groups and their content, as determined by ^{1}H NMR spectroscopy (Table 1), increases as the amount of 10-undecenol does.

Table 1. Synthesis and characterization details of the studied polyols.

Polyol	2:1 Ratio	$\overline{M}_n$ ($\times 10^3$)[a)]	$\overline{M}_w/\overline{M}_n$[a)]	% Diol[b)]	mmol OH per g[c)]
POH1.5	1.5	3.00	6.23	9	1.36
POH2	2	2.67	4.67	12	1.76
POH3	3	2.07	2.91	16	2.27
POH5	5	1.71	2.42	24	2.94
POH8	8	1.39	1.81	31	3.40

[a)]Determined by SEC; [b)]percentage of 10-undecenol self-metathesis as determined by GPC analysis; [c)]hydroxyl value as determined by ^{1}H NMR.

The metathesis polymerizations were also monitored by ^{1}H-NMR spectroscopy (Figure 2). Terminal double bond signals (5.8 and 4.9 ppm) disappeared for the five formulations (compare Table 1), and a signal corresponding to the internal double bonds formed in the metathesis reaction appeared at 5.4 ppm. Signals below 1ppm attributable to methyl groups were observed, which can be explained by isomerization of the terminal double bond to internal ones.[18] Thus, the obtained polyols contain some nonfunctionalized branch ends, which would remain as dangling chains in the final cross-linked polyurethanes.

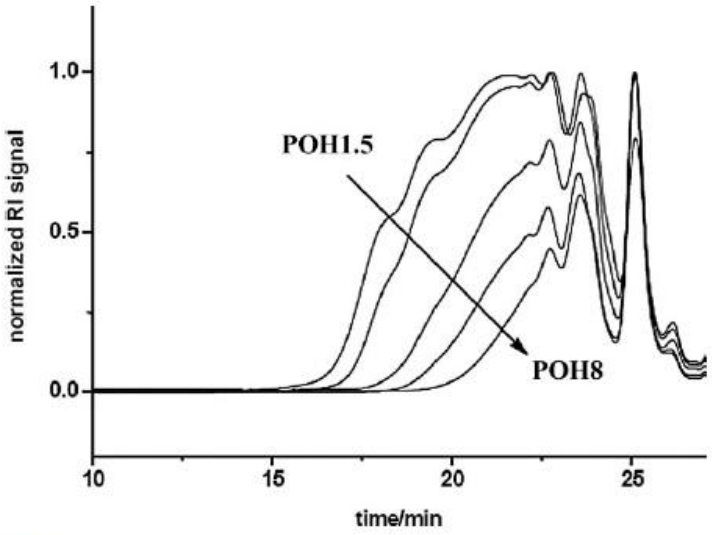

Figure 1. SEC traces of the prepared polyols POH1.5–POH8 (see Table 1).

The DSC curves of these polyols show several endothermic peaks (Figure 3) that should be ascribed to the presence of different oligomers or crystalline forms. For the polyols with lower proportion of chain stopper, the endothermic

peaks are observed between 0 and 40 ºC, while for those synthesized with a higher content of 10-undecenol, a sharp endothermic peak appears at around 50 ºC. According to the higher percentage of self-metathesis of chain stopper, this peak could be attributed to the melting of the linear diol originated in the self -metathesis of 10-undecenol.

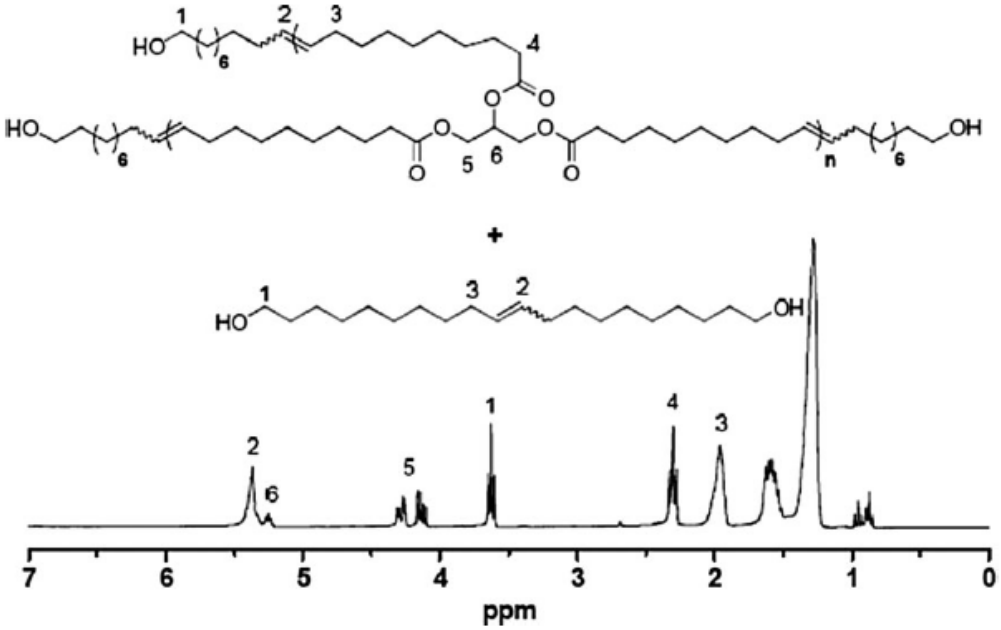

Figure 2. ^{1}H NMR with peak assignment of polyol POH2 (see Table 1).

Polyurethanes were then synthesized from the above described polyols by dissolving the reactants, in the desired stoichiometry, in anhydrous toluene and under argon atmosphere. The reactant solutions were mixed, casted over a silanized glass plate preheated to 70 ºC, cured at 70 ºC for 2 h and post-cured at 120 ºC for 3 h.

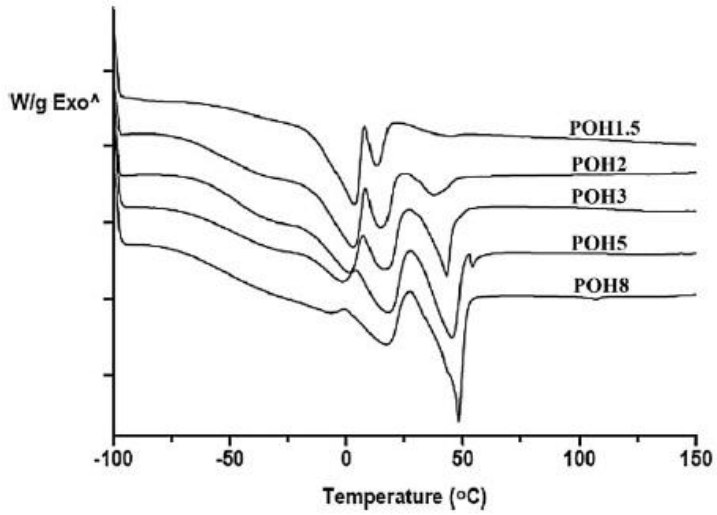

Figure 3. Differential scanning calorimetry (DSC) traces (20 °C·min^{-1}) of polyols POH1.5–POH8 (compare Table 1).

Characterization of the polyurethanes by FTIR/ATR showed the disappearance of the isocyanate and hydroxyl stretching bands at 2240 and 3370 cm^{-1}, respectively. New bands appeared due to the urethane group: the stretching of N–H bonds at 3353cm^{-1} and of the C=O bonds, which is partially overlapped with the carbonyl band of the fatty acid moiety, at 1738 cm^{-1}. The intensity of these bands increase as the hydroxyl content of the starting polyol does, as expected. The thermal behavior of the polyurethanes was investigated by DSC (Figure 4, Table 2). They show glass

transition temperatures below 0 ºC that increase as the hydroxyl content increases, in accordance with a higher degree of cross-linking. Moreover, the lower molecular weight of the polyol and the higher percentage of the diol cause a restriction of segmental mobility, increasing Tg values and hindering the detection of Tg by DSC for PU8. Moreover, as a result of the higher hydroxilic content of the starting polyol, melting endotherms appear in the DCS plots. Since the starting material in the preparation of the polyurethanes is a mixture of polyol and diol, structurally inhomogeneous systems containing various domains with different sizes are obtained, which consist of alternate polyol or diol isocyanate sequences. Parts of the domains are chemically cross-linked with covalent bonds between polyol and isocyanate and others are physically crosslinked due to the linear diol-isocyanate segments via hydrogen bonding. The chemical cross-links would reduce the mobility of molecular chains and restrict the effective packing into crystals. When increasing amounts of the shorter diol are employed, the effective packing of polymer chains into crystals seems to be promoted and semicrystalline materials are obtained.

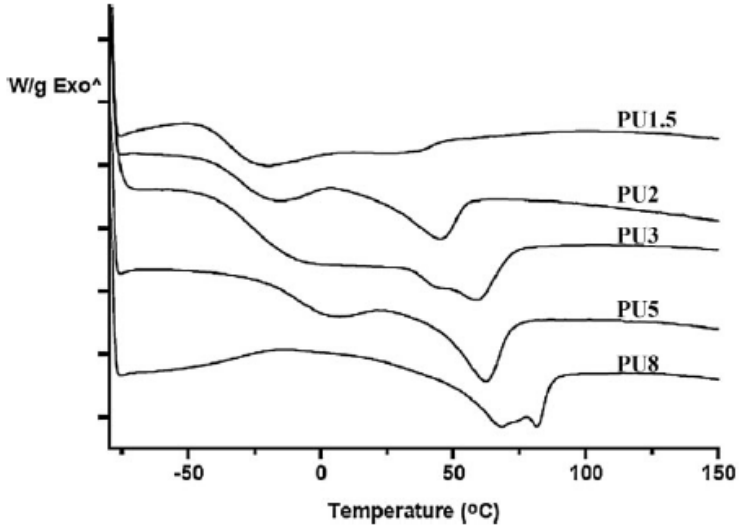

Figure 4. Differential scanning calorimetry (DSC) traces of polyurethanes (20 °C·min^{-1}) that were obtained from polyols POH1.5–POH8 (see Table 1) with MDI.

The thermal stability of the polyurethanes in nitrogen atmosphere was studied by TGA (Table 2). The shapes of the weight-loss curves show the typical degradation behavior of polyurethanes. Differences in thermal stability appear to be small and the decomposition takes place at ca. 280 ºC.

Table 2. Thermal properties of the prepared polyurethanes.

PU	T_g [°C][a)]	T_m [°C]	ΔH [J·g^{-1}]	T_g [°C][b)]	$T_{5\%}$ [°C][c)]	Yield $_{800}$ °C [%]	T_{max} 1 [°C][d)]	T_{max} 2 [°C][d)]	Stress [MPa]	Strain [%]	Young's modulus
PU1.5	−34	–	–	−7	288	7	298	457	1.2	65	3.4
PU2	−28	45	5	−4	288	8	296	461	3.1	150	7.6
PU3	−24	59	7	−1	287	10	293	465	5.5	174	23
PU5	−5	62	8	13	281	10	290	466	7.6	198	38
PU8	–	81	13	13	276	10	289	465	9.1	265	61

[a)] 1/2 ΔCp from DSC data; [b)] $\tan\delta_{max}$ from DMTA data; [c)] temperature of the 5% of weight loss; [d)] temperature of the maximum weight loss.

There is a first weight loss (related to the decomposition of urethane bonds) that increases as the hydroxyl content of the polyol increases, in accordance to the existence of a higher amount of weaker urethane bonds. The main decomposition process is related to the polyol chain scission above 450 ºC.

Dynamic mechanical thermal analysis (DMTA) of the polyurethane films was performed between 90 and 150 ºC. In Figure 5, storage modulus curves for the PUs are presented. All polyurethanes showed two transitions, which can be related to the already discussed DSC traces. The first drop in the storage modulus, assigned to the glass transition of the materials, appears close to 0 ºC. The second transition, originated by melting of the crystalline domains, is centered at 55 ºC for PU1.5 and PU2, while it is close to 75 ºC for all other studied PUs. Both transitions are shifted from lower

temperatures for PU1.5 to higher for PU8. Moreover, the intensities of the steps are different for each sample: PU1.5 has a first main transition below 10 ºC with a small step close to 55 ºC. Upon increase of the diol proportion in the polyurethane, the second step becomes more important, which is in agreement with the fact that the crystalline phase is originated by reaction of the diol obtained by self-metathesis of 2 with MDI. The storage modulus value in the rubbery plateau increases with the increment of the diol proportion, according to a lower crosslinking density.

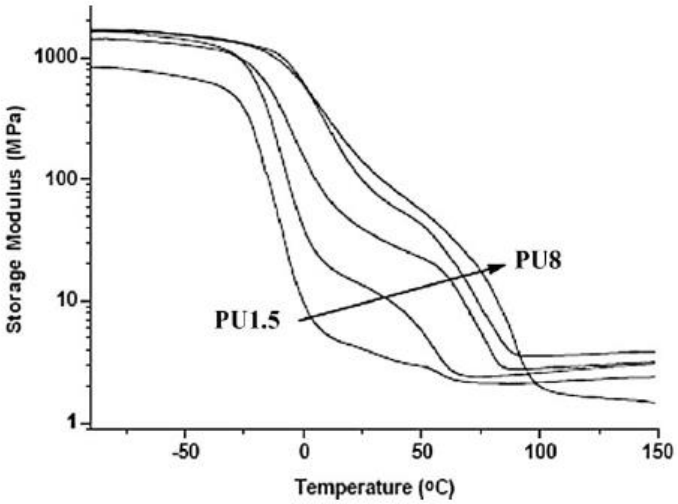

Figure 5. Storage modulus of the prepared polyurethanes.

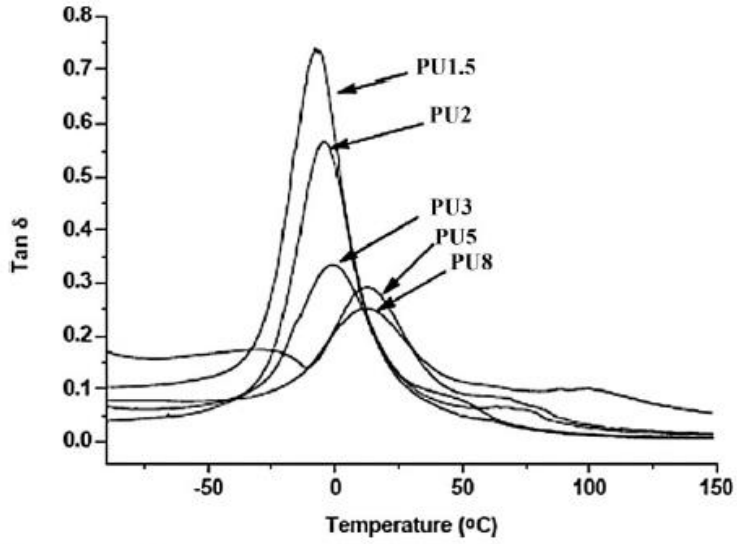

Figure 6. Tanδ and loss factor of the prepared polyurethanes.

The maximum of the tanδ curves was used to determine the glass transition of the polyurethanes. Figure 6 shows that the maximum of the curve moves from 7 ºC for PU1.5 to 13 ºC for PU8 (Table 2). These values, assigned to the glass transition, are in good agreement with the tendency observed by DSC. The shape of the peak gives information about the cross-linking density; thus, for PU1.5 the highest and sharpest peak indicates a lower cross-linking, whereas PU8 showed the lowest and broadest peak indicating that the cross-linking density is higher. This behavior is due to both, covalent cross-linking points for urethane bonds and crystalline domains, which also act as net points.

Figure 7 shows the stress–strain curves for the different polyurethanes. PU1.5 presented the lowest values for the stress applied at break, final strain and Young's modulus. By increasing the diol proportion (and therefore the crystalline phase of the polyurethane), the resistance of the film is improved. Thus, the maximum stress for PU1.5 was of 1.2 MPa, much lower than that of the PU8 which is 9.1 MPa. In the same way, the percentage of strain at the break for PU1.5

was 65%, while it was above 250% for PU8. The other polyurethanes showed intermediate values as can be seen in Table 2.

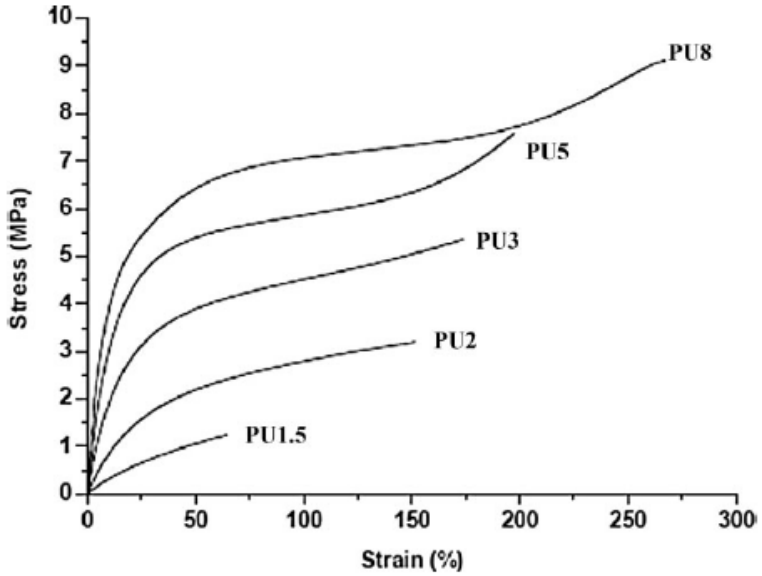

Figure 7. Stress–strain plots of the investigated polyurethanes.

The obtained polyurethanes showed a shape-memory effect, which was quantified by applying the cyclic tensile tests described in the experimental part. Samples were heated above the switching temperature and stretched to the desired temporary shape. In the next step, the materials were cooled down to 25 ºC to fix the temporary shape and shape recovery was triggered by heating the sample above the transition temperature. The tensile test was performed for three consecutive runs on the same sample and the strain fixity rate Rf and the strain recovery rate Rr were calculated (Table 3).

$$R_f(N) = \frac{L_u(N)}{L_m(N)} \times 100\% \quad (2)$$

$$R_r(N) = \frac{L_m(N) - L_f(N)}{L_m(N) - L_f(N-1)} \times 100\% \quad (3)$$

where Lu is the fixed strain of the film unloaded and stabilized at 25 ºC, Lm the strain of the polyurethane before release of the stress, Lf the final strain of the sample at 100 ºC , and N is the number of cycles. Rr indicates the quality of the restoration of the primary shape after reheating and Rf expresses how well the material can maintain the total strain of the secondary shape after releasing the force on the sample, thus, ideal values for Rf and Rr are 100%.

Table 3. Shape memory properties of the prepared polyurethanes.

	R_f			R_r			Stress [MPa]	Strain [%]
	Cycle 1	Cycle 2	Cycle 3	Cycle 1	Cycle 2	Cycle 3		
PU3	70	76	75	79	95	94	0.8	110
PU5	75	78	80	89	98	98	0.8	120
PU8	92	95	95	92	98	99	0.5	140

Polyurethanes PU1.5 and PU2 showed no capability to fix strain, while polyurethanes PU3, PU5, and PU8 showed a shape-memory effect (Figure 8). For PU3, the force ramp applied to the film produces a different final strain (Lm)

for each cycle. It is clear that the second and third cycles are quite similar, and indicate a clear Rr and Rf improvement compared to the first one. This small training effect is due to the occurrence of some chain relaxation during the mechanical cycle, which is characteristic of SMPs.[19] For PU5 and PU8 the three consecutive thermomechanical cycles are superimposable. Both the shape fixing and shape recovery increased significantly for PU5. PU8 showed almost complete shape fixing and recovery, as can also be seen from the high Rf and Rr values that were almost unchanged through the cycles.

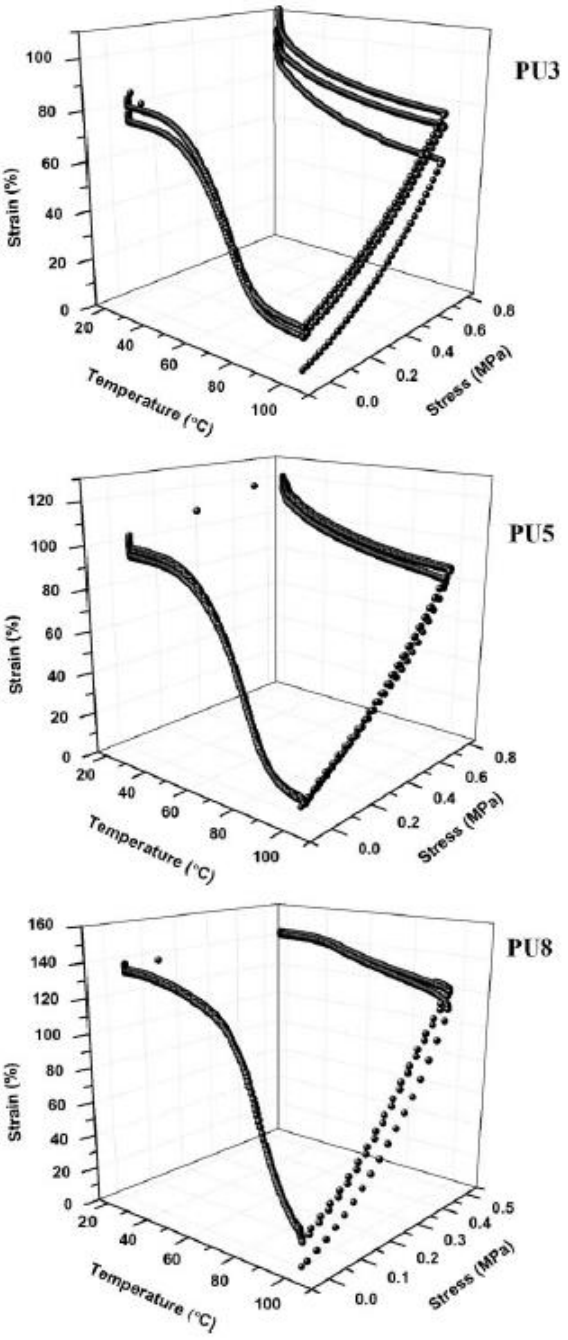

Figure 8. Shape-memory cycles of the investigated polyurethanes.

Since the obtained polyurethanes are covalently cross-linked semicrystalline networks, the secondary shape is fixed by crystallization while the permanent shape is established by chemical crosslinking. The improvement on the shape memory properties from PU3 to PU8 can be related to a lower cross-linking density and a higher percentage of diol, which would increase the physical cross-links that keep the material in its secondary shape.

Conclusion

Branched polyols were prepared via a one step one pot procedure by applying acyclic triene metathesis polymerization to a triglyceride. By using different amounts of a chain stopper in combination with this triglyceride, polyols of varying molecular weight and OH value could be obtained. Using these polyols, novel renewable polyurethanes were prepared by reacting them with MDI. The resulting polyurethanes were fully characterized and their mechanical properties were investigated in detail. Some of poly- the covalently cross-linked semicrystalline networks obtained showed good shape memory properties

Acknowledgements: The authors express their thanks to MICINN (Ministerio de Ciencia e Innovación, MAT2008-01412) for the financial support for this work.

Keywords: ATMET; metathesis; polyurethanes; renewable resources; shape memory

[1] [1a] M. N. Belgacem, A. Gandini, Monomers, Polymers and Composites from Renewable Resources, Elsevier, Oxford 2008; [1b] M. A. R. Meier, J. O. Metzger, U. S. Schubert, Chem. Soc. Rev. 2007, 36, 1788; [1c] J. O. Metzger, Eur. J. Lipid Sci. Technol. 2009, 111, 865.

[2] T. M. Trnka, R. H. Grubbs, Acc. Chem. Res. 2001, 34, 18.

[3] [3a] A. Rybak, P. A. Fokou, M. A. R. Meier, Eur. J. Lipid Sci. Technol. 2008, 110, 797; [3b] M. A. R. Meier, Macromol. Chem. Phys. 2009, 210, 1073.

[4] [4a] A. Rybak, M. A. R. Meier, Green Chem. 2007, 9, 1356; [4b] A. Rybak, M. A. R. Meier, Green Chem. 2008, 10, 1099; [4c] R. Malacea, C. Fischmeister, C. Bruneau, J.-L. Dubois, J.-L. Couturier, P. H. Dixneuf, Green Chem. 2009, 11, 152.

[5] [5a] L. Montero de Espinosa, J. C. Ronda, M. Galia, V. Cadiz, M. A. R. Meier, J. Polym. Sci., Part A: Polym. Chem. 2009, 47, 5760; [5b] L. Montero de Espinosa, M. A. R. Meier, J. C. Ronda, M. Galia, V. Cadiz, J. Polym. Sci., Part A: Polym. Chem. 2010, 48, 1649.

[6] [6a] J. E. Schwendeman, A. C. Church, K. B. Wagener, Adv. Synth. Catal. 2002, 344, 597; [6b] H. Mutlu, L. Montero de Espinosa, M. A. R. Meier, Chem. Soc. Rev. 2011, 40, 1404. [7] K. B. Wagener, K. Brzezinska, J. D. Anderson, T. R. Younkin, K. Steppe, W. DeBoer, Macromolecules 1997, 30, 7363.

[8] [8a] G. V. Shultz, L. N. Zakharov, D. R. Tyler, Macromolecules 2008, 41, 5555; [8b] K. Terada, E. B. Berda, K. B. Wagener, F. Sanda, T. Masuda, Macromolecules 2008, 41, 6041.

[9] [9a] A. Rybak, M. A. R. Meier, ChemSusChem 2008, 1, 542; [9b] P. P. Matloka, Z. Kean, M. Greenfield, K. B. Wagener, J. Polym. Sci., Part A: Polym. Chem. 2008, 46, 3992; [9c] K. R. Brzezinska, K. B. Wagener, G. T. Burns, J. Polym. Sci., Part A: Polym. Chem. 1999, 37, 849.

[10] P. A. Fokou, M. A. R. Meier, Macromol. Rapid Commun. 2008, 29, 1620.

[11] U. Biermann, J. O. Metzger, M. A. R. Meier, Macromol. Chem. Phys. 2010, 211, 854.

[12] E. Del Rio, G. Lligadas, J. C. Ronda, M. Galia, M. A. R. Meier, V. Cádiz, J. Polym. Sci., Part A: Polym. Chem. 2010, 49, 518.

[13] C. Liu, H. Qin, P. T. Mather, J. Mater. Chem. 2007, 17, 1543.

[14] [14a] K. Otsuka, C. M. Wayman, Shape Memory Materials, Cambridge University Press, New York 1998; [14b] A. Lendlein, S. Kelch, Angew. Chem., Int. Ed. 2002, 41, 2034.

[15] P. T. Mather, X. Luo, I. A. Rousseau, Annu. Rev. Mater. Res. 2009, 39, 445.

[16] M. Behl, A. Lendlein, Mater. Today 2007, 10, 20.

[17] A. Lendlein, R. Langer, Science 2002, 296, 1673.

[18] [18a] B. Schmidt, Eur.J. Org. Chem. 2004, 1865;

[18b] B. Schmidt, J. Mol. Catal. A 2006, 254, 53.

[19] J. E. Gautrot, X. X. Zhu, Macromolecules 2009, 42, 7324.